THE AMERICAN SOCIETY OF MECHANICAL ENGINEERS
Three Park Avenue, New York, N.Y. 10016-5990

99-GT-175

ANALYSIS OF ACTIVELY CONTROLLED COULOMB DAMPING FOR ROTATING MACHINERY

John M. Vance
Luis A. San Andrés

Mechanical Engineering Department
Texas A&M University
College Station, Texas, 77843-3123

ABSTRACT

Attempts have been made in the past to use Coulomb damping for vibration suppression in rotating machinery. Typically, a dry friction damper is designed to operate on a flexible bearing support. These designs have usually been unsuccessful in practice, partly because the Coulomb coefficient changes with temperature, with ingress of dirt or lubricant, and with the surface wear conditions. It is known that purely Coulomb damping forces cannot restrain the peak rotor whirl amplitudes at a critical speed. The invention of a disk type of electroviscous damper, utilizing a fluid with electrorheological (ER) properties, has recently revived the interest in Coulomb type dampers. Several investigations have suggested that a Coulomb friction model was the best representation for an ER damper with voltage applied. This model was used to study the feasibility of developing actively controlled bearing dampers for aircraft engines. This paper analyzes the imbalance response of two different rotordynamic models with Coulomb friction damping and shows the benefit of adding active control. Control laws are derived to achieve minimum rotor vibration amplitudes while avoiding large bearing forces over a speed range that includes a critical speed. The control laws are derived for purely Coulomb type of damping and assuming a combination of Coulomb and viscous damping effects. It is shown that the most important feature of Coulomb damping for minimal rotordynamic amplitude response is the control of rotor support stiffness, i.e. leading to the relocation of critical speeds, rather than control of a damping coefficient.

NOMENCLATURE

C_1, C_2	support viscous damping coefficient, ½ viscous damping coefficient at rotor midspan.
C_{eq}	$\lvert F_C/\omega X \rvert$; equivalent viscous damping coefficient for Coulomb friction.
d_C	$\lvert F_C / K_s u \rvert$; dimensionless Coulomb damping parameter.
F_C	constant friction force of Coulomb damper, $f_C=2F_C$
F_T	transmitted force to foundation.
K_1 , K_s	support stiffness, ½ shaft stiffness, $k=2K_1$
M_1 , M_2	support mass, ½ modal mass of rotor, $m=2M_2$
r_1, r_2	dimensionless amplitudes of motion at support and rotor midspan
T	$F_T/M_2 u\omega^2$, transmissibility ratio.
t	time.
u	imbalance (rotor mass eccentricity).
U_1, U_2, V_1, V_2	coefficients defined in equation 11.
X_1, X_2	support and rotor displacements in X direction.
Y_1, Y_2	support and rotor displacements in Y direction.
α	M_1/M_2, ratio of support mass to ½ rotor mass.
β	K_1/K_s, ratio of support to rotor stiffness.
Δ	$\left(1-\overline{\omega}^2\right)\left(1+\beta-\alpha\overline{\omega}^2\right)-1$, characteristic equation of undamped rotor- support system.
ϕ_1, ϕ_2	phase angles at support and rotor.
ζ_1, ζ_2	$C_1/2\sqrt{K_1 M_2}$, $C_2/2\sqrt{K_s M_2}$, viscous damping ratios at support and rotor midspan.
ω	rotor spin frequency.
ω_n	$\sqrt{k/m}$, rigid rotor natural frequency on flexible bearing supports.
ω_s	$\sqrt{K_s / M_2}$, flexible rotor natural frequency on rigid supports.
$\omega_{1,2}$	flexible rotor system undamped critical speeds.
ω_b	$d_C^{1/2}(1 + d_C)^{1/2}$, break-loose frequency for start of coulomb damper action.
$\omega_{a1,2}$	frequencies of intersection for identical rotor amplitudes.
$\omega_{b1,2,3}$	frequencies of intersection for identical transmitted forces.
$\overline{\omega}$	ω/ω_s , dimensionless frequency.

INTRODUCTION

Coulomb (dry friction) dampers for vibration suppression in rotating machinery have been used in the past, and typically designed to operate on a flexible bearing support. However, these designs were unsuccessful in practice, mainly due to the changes of dry friction coefficient changes with temperature, ingress of dirt or lubricant, and the inevitable wear of the contact surfaces. A particularly unfortunate example of these shortcomings occurred early in the SSME turbopump design and development as described by Ek (1981). In 1988 an interest in Coulomb damping was revived by the invention of a disk type of electroviscous damper utilizing fluid with electrorheological

Presented at the International Gas Turbine & Aeroengine Congress & Exhibition
Indianapolis, Indiana — June 7–June 10, 1999

properties, see Nikolajsen and Hoque (1990), and modeled as a dry friction type device. Vance, et al. (1999a) detail a further study to determine the feasibility of developing actively controlled bearing dampers for aircraft engines, and the ER damper became a candidate for consideration.

Kollias and Dimaroganus (1992) analyzed an ER damper using experimental data from the test rig of Nicolajsen and Hoque. In deriving equations for the damping force, Kollias amd Dimaroganus state that "although the velocity of the disk is changing with time, a quasi-static approach to the Navier-Stokes equations is valid at time (t)." Consequently these authors ignore the velocity dependence of the damper force, and finally conclude that it is of the Coulomb friction type. An equivalent viscous damping coefficient from Den Hartog (1956) is used to represent Coulomb friction force and to predict the rotor motion. However, this equivalent coefficient is derived for planar harmonic vibration and is not quantitatively correct for rotordynamic applications. Nonetheless, since the value of damping coefficients are seldom known accurately in any case, the major drawback of using an equivalent viscous coefficient is a gross under prediction of whirl amplitudes at critical speeds unless the frequency dependence of the coefficient is included. If residual viscous damping is present, as it usually is in real systems, then the measured resonant amplitude in experiments may actually be limited and the effect incorrectly attributed to the dry friction.

This paper shows that a damper with Coulomb (dry friction) properties becomes much more viable as a bearing damper for rotating machinery if the Coulomb coefficient can be actively controlled and if the residual viscous damping is small. In companion papers, Vance, et al. (1999) detail the feasibility study on actively controlled dampers for aircraft engines, and Vance and Ying (1999) report relevant experimental measurements from a rotordynamic test rig with an ER damper.

COULOMB DAMPING IN ROTATING MACHINES

Den Hartog (1956) described an exact solution for the response of a spring mass system excited by a harmonic force $(F \sin(\omega t))$ and damped by a Coulomb friction force F_C. In an approximate analysis of planar vibration, $x(t) = X \sin(\omega t)$, Den Hartog deduced that the energy dissipated over a full cycle of motion by the constant (Coulomb) friction force (F_C) is $(4F_CX)$. Equating this to the energy per cycle dissipated by a viscous damping force yields an equivalent viscous coefficient, $C_{eq} = (4F_C/\pi\omega X)$. This suggests that the solution of the linear equations of motion with viscous damping can be used to predict qualitatively the response of a system with Coulomb damping. Note that with viscous damping, the system amplitude of response is bounded at resonance, i.e. at the system natural frequency. However, Hartog also reveals that since the derived C_{eq} is frequency dependent it actually results in an infinite amplitude response at a resonance. In a later textbook, Steidel (1989) also shows that the response of a Coulomb-damped vibrating system is infinite at resonance, so that the indiscriminant use of C_{eq} (as if the system was linear) would lead to serious errors in the predicted amplitudes of response around a critical speed.

None of this, however, is exactly correct for a rotating system describing orbital motions. For example, it is simple to demonstrate that the energy dissipated by a Coulomb friction force in one full period of a circular orbit (of radius X) is $(2\pi XF_C)$, and not $(4F_CX)$ as the planar motions shows. The correct equivalent viscous coefficient for circular centered orbits is $C_{eq} = (F_C/\omega X)$. The analytical solution given below for orbital motion also shows that Coulomb friction alone cannot restrain the amplitude of a rotating machine at its critical speed. The ER damper tests reported by Nikolajsen and Hoque (1990), and those presented later by Vance and Ying (1999) all show finite amplitudes of rotor motion at the critical speeds (even without active control), which indicates that some other type of damping is present in those tests.

TWO ROTOR MODELS FOR THE ROTORDYNAMIC ANALYSIS OF A COULOMB DAMPER

Any real system has some amount of residual viscous damping, both in the supports (e.g. from structural hysteresis or from unsolidified ER fluid) and on the rotor (e.g. from aerodynamics). Each of the two authors developed independently a simplified model for the rotordynamic analysis of a rotor supported on ER dampers and in order to derive appropriate control strategies. Model 1 considers a simple rotor on flexible supports and accounts for the constant Coulomb force without an equivalent viscous damping action. Model 2 corresponds to a flexible rotor mounted on massive flexible supports where the Coulomb dampers are located and idealized with equivalent viscous damping coefficients. It is important to note that both models lead to the same conclusions and recommendations.

Model 1: Rigid rotor on flexible supports with Coulomb forces

Figure 1 shows a modified Jeffcott rotor of mass $(2M_1)$ supported on bearings with stiffness (K_1) (Barrett et al., 1978, Vance 1988). The elastic and Coulomb damping forces acting on the rotor while executing steady-state circular orbits are depicted in Figure 2. A Coulomb force (F_C) is applied at each bearing, in parallel with the bearing support stiffness (K_1). For a low enough ratio of bearing support stiffness to shaft stiffness, the model will act approximately as a rigid rotor except when the bearing supports are locked up (seized) by a large Coulomb friction force. If the bearings lock up the shaft bends and the flexible rotor system will show a higher critical speed. In the locked up-mode the rotor system is assumed to have a viscous damping ratio $\zeta_2 = .015$, a value typical for steel machinery with no ancillary damping. This simple model, with appropriate mass, stiffness and damping parameters, is representative of the test rig with a cantilevered rotor as described by Vance and Ying (1999).

Let $k = 2K_1$, $m = 2M_1$ and $f_c = 2F_C$, and using Newton's Second Law in radial and tangential (polar) coordinates (r,t), the dynamic equilibrium equations in the radial and tangential directions for an imbalance displacement (u) are given by,

$$k r = m\left(\omega^2 r + \omega^2 u \cos(\phi)\right) \tag{1}$$

$$-2F_C = -f_C = -m\omega^2 u \sin(\phi) \tag{2}$$

Combination of equations (1) and (2) gives,

$$f_C^2 + \left(k - m\omega^2\right)^2 r^2 = \left(m\omega^2 u\right)^2 \tag{3}$$

and from this, the solution for the orbit amplitude (r) is equal to

$$r = \frac{m\omega^2 u \sqrt{1 - \left(\dfrac{f_C}{m\omega^2 u}\right)^2}}{\left(k - m\omega^2\right)} \tag{4}$$

Note that the argument of the radical becomes negative when the Coulomb friction force (f_C) is larger than the amplitude of the unbalance force. Under this condition the bearings are locked up, the solution for the amplitude (r) is invalid, and the flexible rotor model

mounted on hard supports then prevails. (Model 2 details more about this operating condition) Note also that the amplitude is unbounded at resonance for any nonzero Coulomb damping force less than the lockup value. Thus, a purely Coulomb damping force cannot restrain the amplitude at the critical speed. If a real rotating machine is observed to have finite peak amplitude at its critical speed, then some type of damping other than Coulomb must be present. Another form of equation (4) with $\omega_n = \sqrt{k/m}$ is,

$$\frac{r}{u} = \frac{\left[\left(\frac{\omega}{\omega_n}\right)^4 - \left(\frac{f_C}{ku}\right)^2\right]^{1/2}}{1 - \left(\frac{\omega}{\omega_n}\right)^2} \qquad (5)$$

Inspection of equations (4) and (5) reveals two different expressions for the break loose speed (ω_b) where the unbalance force becomes large enough to initiate sliding and the Coulomb friction becomes active as an energy dissipator, i.e.

$$\omega_b \geq \omega_n \sqrt{\frac{f_C}{ku}} = \sqrt{\frac{f_C}{mu}} \qquad (6)$$

The first expression above shows that if $F_C > (K_1 u)$ the damper will not break loose and become operational until the resonance speed has been exceeded. Then equations (4) or (5) govern the amplitude of rotor response. Below the break-loose speed (ω_b) the bearings will be locked up and the rotor will bend with no damping contribution from the bearings. If $F_C < (K_1 u)$, an unbounded amplitude at resonance will occur unless some other type of damping (e.g. viscous) is present or unless active control of the friction force is implemented as described below.

Control laws for Coulomb friction combined with residual viscous damping acting at both the supports and the rotor

The control law for rotor model 1 is very simple and relies on the ability of the Coulomb friction forces to lock and unlock the supports, and thus, shift the critical speed. During rotor acceleration the friction force (F_C) is kept active at a value larger than ($K_1 u$), see equation (6), up to a speed above the unlocked critical speed, and then turned off at a speed below the locked critical speed. Here "locked" and "unlocked" refer to the freedom of the shaft to move at the bearing (and friction damper) location. Predictions follow for system parameters based on the ER-damped rotordynamic test rig used by Vance and Ying (1999), see Table 1. Figures 3 and 4 show the Bode plots for the rotor amplitude of response without a damper and with a Coulomb damper with on-off schedule as determined from the control law. The unlocked and locked critical speeds are 5576 rpm and 8395 rpm, respectively. In Figure 3 the baseline imbalance response with no Coulomb friction corresponds to a small residual viscous damping (ζ_1=0.05) at the supports. The other curve shows how the rotor response curve changes when a 178 N (40 lb) Coulomb friction force is applied at the supports over the speed range to 7100 rpm and then turned off. In Figure 4 the baseline rotor has a much larger residual viscous damping ratio (ζ_1=0.25) in the supports.

Note how the rotor response changes when the Coulomb friction is applied with the same control law. It can be seen that the actively controlled Coulomb friction is much less effective on the system with large residual viscous damping, i.e. there is only a small reduction of amplitudes around the unlocked critical speed and the peak rotor amplitude is actually larger. Furthermore, the system with larger residual viscous damping will have higher dynamic bearing forces at high speeds along with a shorter bearing life (Vance, 1988). Unfortunately, the ER damper tested by Vance and Ying (1999) had a large residual viscous damping even with no voltage applied across the ER fluid. This appears to be a characteristic of most ER fluids that could be used in Nikolajsen device.

Model 2: Flexible rotor and supports with combined viscous and Coulomb damping.

Figure 5 depicts the second model for a modified Jeffcott rotor mounted on flexible and massive supports. The bearing supports provide stiffness with combined viscous and Coulomb damping representing the ER damper. At the rotor middle span the damping is regarded as viscous. Neglecting angular acceleration, disk gyroscopic effects, internal rotor damping and cross-coupled effects on the rotor and supports, the governing equations of motion in complex notation are:

$$\begin{aligned} M_2 \ddot{Z}_2 + K_s (Z_2 - Z_1) + C_2 \dot{Z}_2 &= M_2 u\omega^2 e^{i\omega t} \\ M_1 \ddot{Z}_1 + K_s (Z_1 - Z_2) + K_1 Z_1 + C_1 \dot{Z}_1 + C_c \dot{Z}_1 &= 0 \end{aligned} \qquad (7)$$

where $Z_1 = X_1 + iY_1$, $Z_2 = X_2 + iY_2$, are the complex dynamic displacements at the bearing support and at the rotor middle span, respectively. Refer to the Nomenclature for a proper definition of all the parameters. C_1 and C_2 are viscous damping coefficients at the support and middle disk, respectively; and $C_C = F_C / \left(\omega \left|Z_1\right|_{max}\right)$ is the equivalent viscous damping coefficient for Coulomb friction with (F_C) as a constant friction force (Jacobsen, 1930, Den Hartog, 1930).

Consider that the system rotor-supports has been in motion for some time and a "steady state" condition has been reached. The motion satisfies the following conditions:

(a) the frequency of rotor whirl motion is synchronous with that of the imbalance force; and

(b) the motion is continuous without stand stills, i.e., the rotor center and supports describe circular orbits.

The support and rotor displacements are specified as $Z_1 = A_1 u e^{i\omega t}$ and $Z_2 = A_2 u e^{i\omega t}$, where $A_1 = r_1 e^{-i\theta 1}$, $A_2 = r_2 e^{-i\theta 2}$.

The assumptions for the motion lead to a set of algebraic equations for determination of the rotor steady-state motion. In dimensionless form these equations are,

$$\begin{aligned} \left[1 - \bar{\omega}^2 + 2i\zeta_2\bar{\omega}\right] A_2 - A_1 &= \bar{\omega}^2 \\ \left[1 + \beta - \alpha\bar{\omega}_2 + i\frac{d_c}{r_1} + 2i\zeta_1\bar{\omega}\right] A_1 &= A_2 \end{aligned} \qquad (8)$$

where $\bar{\omega} = \omega/\omega_s$ is a frequency ratio with $\omega_s = (K_s/M_2)^{1/2}$ as the natural frequency of the flexible rotor on rigid supports. The parameters $\alpha = M_1/M_2$, $\beta = K_1/K_s$ denote the support mass and rigidity ratios, and ζ_1, ζ_2 are damping ratios at the supports and rotor midspan, respectively. The parameter $d_C = (F_C/K_s u)$ denotes the dry-friction damper of magnitude inversely proportional to the imbalance (u). The undamped critical speeds, natural frequencies (ω_1, ω_2), of the rotor-support system are determined from equations (8) as:

$$\overline{\omega}_{1,2} = \left[\frac{(1+\beta+\alpha)}{2\alpha} \mp \frac{1}{2\alpha} \sqrt{(1+\beta+\alpha)^2 - 4\alpha\beta} \right]^{1/2} \qquad (9)$$

Straight forward manipulations of equations (8) renders the amplitude response (r_1) at the supports as (equation 10):

$$r_1 = \frac{-(V_1U_1 + V_2U_2) + \sqrt{(V_1U_1 + V_2U_2)^2 - (V_1^2 + V_2^2)(U_1^2 + U_2^2 - \overline{\omega}^4)}}{V_1^2 + V_2^2}$$

where $V_1 = \Delta - 4\zeta_1\zeta_2\overline{\omega}^2$;

$$V_2 = 2\zeta_2\overline{\omega}(1+\beta-\alpha\overline{\omega}^2) + 2\zeta_1\overline{\omega}(1-\overline{\omega}^2) \qquad (11)$$

$$U_1 = -2\zeta_2\overline{\omega}\, d_c; \qquad U_2 = d_c(1-\overline{\omega}^2)$$

and $\Delta = (1-\overline{\omega}^2)(1+\beta-\alpha\overline{\omega}^2) - 1$, is the characteristic polynomial for the undamped rotor-support system.

The amplitude at the supports must be real valued and positive, i.e. $r_1 \geq 0$. However, for frequencies less than a "break loose" frequency (ω_b) for sliding to occur, r_1 is imaginary and physically it must then be equal to zero. For low frequency operation ($<\omega_b$) the Coulomb force is rather large, preventing any support motion, and the rotor system acts as if on rigid supports. Letting r_1 be equal to zero in equation (10) renders the value of the break-loose frequency as:

$$\omega_b = \omega_s \frac{d_C^{1/2}}{(1+d_C)^{1/2}} \qquad (12)$$

The frequency (ω_b) determines the operating condition when the elastic shaft force equals the Coulomb force, i.e. $K_s Z_2 = F_C$. If no Coulomb friction is present, $d_C = 0$ and $\omega_b = 0$, while if the friction is too large, $d_C \to \infty$, and ω_b approaches the rigid support critical speed but does not exceed it. For non-null support amplitude motions, the dimensionless amplitude of rotor motion (r_2) and phase angles of response are given by:

$$r_2 = \frac{\left[\overline{\omega}^4 + r_1^2 + 2r_1\overline{\omega}^2 \sin\phi_1 \cos\phi_1\right]^{1/2}}{\left[(1-\overline{\omega}^2)^2 + (2\zeta_2\overline{\omega})^2\right]^{1/2}} \qquad (13)$$

$$tg\ \phi_1 = \frac{V_2 r_1 + U_2}{V_1 r_1 + U_1}; \qquad (14)$$

$$tg\ \phi_2 = \frac{2\zeta_2\overline{\omega}(\overline{\omega}^2 + r_1 \cos\phi_1) + (1-\overline{\omega}^2) r_1 \sin\phi_1}{(\overline{\omega}^2 + r_1\cos\phi_1)(1-\overline{\omega}^2) - 2\zeta_2\overline{\omega}\, r_1 \sin\phi_1}$$

The transmitted force to the base is $F_T = K_1 Z_1 + (C_1 + C_c)\dot{Z}_1$, and the transmissibility ratio is given by:

$$T = \frac{F_T}{M_2 u\omega^2} = \frac{r_1\left[\beta^2 + (2\zeta_1\overline{\omega} + d_c/r_1)^2\right]^{1/2}}{\overline{\omega}^2} \qquad (15)$$

Examples of the dynamic response of rotordynamic Model 2

Consider now a rotor and support system with mass and stiffness ratios equal to $\alpha = 0.25$ and $\beta = 0.5$, respectively. The undamped flexible support natural frequencies are $\omega_1 = 0.546\ \omega_s$ and $\omega_2 = 2.59\ \omega_s$. The viscous damping ratio at the supports (ζ_1) and at the rotor midspan (ζ_2) are equal to 0.075 and 0.001, respectively. Figures 6, 7 and 8 depict, for two Coulomb parameters, $d_C = 0$, 0.15 and 0.5, the amplitude response at the supports and rotor midspan and the transmissibility ratio, respectively. The dashed line curves represent the response for rigid supports, $d_C \to \infty$, i.e. for minimal values of disk imbalance (u) or very large dry friction forces (F_C). Table 2 shows the peak amplitude responses and break-loose frequencies for the two dry friction parameters. Figure 6 shows that the support amplitude without dry friction ($d_C = 0$) is the largest for the entire speed range selected. For the largest coulomb parameter, $d_C = 0.5$, the break-loose frequency to ensue motion at the support is larger than the first flexible support critical speed ω_1, thus eliminating the appearance of the first system resonance.

Figure 7 shows the rotor midspan amplitude of motion (r_2) versus rotor speed. Dry friction forces reduce considerably the amplitude at the midspan well below and above the rigid support critical speed Note that the optimum rotor response is obtained for speeds below the break frequencies where the system behaves as rigidly supported. In operating regions close to the rigid support critical speed (ω_s), the rotor amplitude with combined dry friction and viscous damping actions is larger than with only viscous dampers ($d_C = 0$), and it approaches the rigid support response as $d_C \to \infty$. Figure 8 indicates that transmitted forces well below the rigid support critical speed (ω_s) are reduced considerably for the combined viscous and coulomb damping actions. Lowest transmitted forces are attained for speeds below the break-loose frequency (ω_b) where the system acts as if rigidly supported. However, dry friction increases considerably the transmitted forces for speeds around the rigid support critical speed as well as for speeds larger than the second critical speed of the rotor-flexible support system. At the rigid support critical speed, $\overline{\omega} = 1$, the lowest transmitted forces are obtained without any external damping ($\zeta_1 = d_c = 0$) provided the system has flexible supports.

The rotor middle span amplitude responses intersect at two speeds, below and above ω_s. The transmitted force curves also show three speeds of intersection, the second and third crossings below and above the second critical speed. Note that the intersection points are independent of the level of viscous damping in the system (Timoshenko, 1974, Kirk and Gunter, 1972). The predictions suggest that before the first intersection speed (above ω_1 and below ω_s) the rotor and transmitted force are optimum for the rigid support case ($d_C \to \infty$), which effectively requires rigid supports, i.e. with extremely large dry friction forces or almost null imbalance levels. Fortunately, these stringent conditions are not needed since a maximum coulomb damping coefficient of finite magnitude can be determined by calculating the frequencies at which the flexible support response is equal to the rigid support response. From the amplitude of response curves these frequencies are:

$$\overline{\omega}_{a1,2} = \left[\frac{(1+\alpha+\beta)}{2\alpha} \mp \left\{ \frac{(1+\alpha+\beta)^2 - 4\alpha(\beta+1/2)}{2\alpha} \right\}^{1/2} \right]^{1/2} \qquad (16)$$

while for identical transmitted forces, the intersections occur at

$$\overline{\omega}_{b1,3} = \left[\frac{(1+\alpha+2\beta)}{2\alpha} \mp \left\{ \frac{(1+\alpha+2\beta)^2 - 8\alpha\beta}{2\alpha} \right\}^{1/2} \right]^{1/2},$$

$$\overline{\omega}_{b2} = \left[(1+\alpha)/\alpha\right]^{1/2} \qquad (17)$$

The frequencies (ω_{a1}, ω_{b1}) are above the first critical speed (ω_1); while (ω_{a2}, ω_{b2}) are below the second critical speed (ω_2), and ω_{b3} is above ω_2. The largest coulomb damping parameter is determined by

requiring the break-loose frequency ($\bar{\omega}_b$) to be identical to the frequencies $\bar{\omega}_{a1}$ or $\bar{\omega}_{b1}$. Thus, from equation (12),

$$d_C = \frac{\bar{\omega}_b^2}{1-\bar{\omega}_b^2} \; ; \; \bar{\omega}_b > 1 \qquad (18)$$

For the example (α=0.25, β = 0.5), the intersection frequencies are equal to $\bar{\omega}_{a1} = 0.792$; $\bar{\omega}_{a2} = 2.524$; $\bar{\omega}_{b1} = 0.684$; $\bar{\omega}_{b2} = 2.236$; $\bar{\omega}_{b3} = 2.920$; and the corresponding maximum coulomb friction parameters are $d_{Ca1} = 1.6860$ for $\bar{\omega}_{a1}$, $d_{Cb1} = 0.8825$ for $\bar{\omega}_{b1}$.

Figures 7 through 9 show the rotor amplitude at support and midspan, and transmissibility for the maximum parameters $d_C = 0.882$ and 1.686. For comparison, the cases of $d_C = 0$ (no dry friction) and $d_C = \infty$ (rigid or locked supports) are also included in the figures.

The predictions demonstrate that the lowest derived Coulomb parameter, $d_C = 0.882$ (from matching transmitted force amplitudes) is the one which offers the best rotor response characteristics for most frequencies and when compared to d_C=1.686 or the rigid support case. Note that below (ω_{a1}), the rotor response is identical to the rigid support system since the supports are effectively locked due to the large dry-friction forces. However, in the frequency range above (ω_{a1}, ω_{b1}) and below (ω_{b2}, ω_{b2}) a coulomb damper degrades the rotor-supports system frequency response. (Actually, even viscous damping is of no consequence in this region.) For frequencies above ω_{b3} ($>\omega_2$), the transmitted forces are comparable to those of rigid supports for the coulomb damper parameters considered. For lasting rotor operation, excessive transmitted forces should always be avoided.

As with Model 1, the predictions from Model 2 also suggest that a Coulomb damper could be used as an active device for vibration control of a rotor-support system. This damper, designed to initiate its action at a frequency such that the first system critical speed (ω_1) is effectively eliminated, can then be released at the frequency (ω_{b1}) where the viscous support damping will work up to speeds below or equal to ω_{b2} ($\leq \omega_2$). In the speed range [$\omega_{b1} \leq \omega \leq \omega_{b3}$] the coulomb damper will act again to reduce rotor response and transmitted forces. For supercritical operation, well above ω_2, the coulomb damper would still be active to insure low transmitted forces. The active coulomb damper proposed has the potential of effectively reducing the amplitude of rotor response and transmitted forces over a large range of operating speeds, and if properly controlled it could eventually eliminate all resonances at critical speeds. The simple on-off ("bang-bang") Coulomb damper can control the rotor response over the whole speed range and effectively avoid all system resonances. The effect is similar to the *ER-controlled mass* model of Kollias and Dimaroganus (1992) although our rotordynamic model and its operation are simpler.

CONCLUSIONS

Simple analyses for prediction of the synchronous response of a rotor supported on elastic supports and Coulomb dampers have been presented. The models intend to replicate the prevailing conditions thought to occur with electrorheological fluid dampers. Purely Coulomb (dry) friction without active control cannot restrain the whirl amplitude of a rotating machine at resonance, i.e. the amplitude at the critical speed is unbounded unless some other type of damping is present.

1. The equivalent viscous damping coefficient to represent Coulomb friction in a rotating machine and the analogous coefficient for planar harmonic vibration have different values. For a dry friction damper executing a circular orbit, the correct value is $C_{eq}=F_C/\omega X$ where F_C is the dry friction force.
2. A bearing damper with Coulomb (dry friction) properties becomes much more useful and practical as a bearing damper for rotating machinery if the Coulomb coefficient can be actively controlled and if the residual (viscous) damping is small.
3. Successful control laws for varying the dry friction force rely on shifting the critical speeds (controlling support stiffness) in order to avoid them rather than changing the damping ratio.
4. A general rule for the control law is to use the dry friction force to traverse the soft bearing critical speed and then remove it at supercritical speeds. This will reduce the dynamic forces transmitted to the bearing as well as the rotor whirl amplitude.

Details on relevant experimental results and issues of interest for ER dampers are given in a companion paper (Vance and Ying, 1999).

ACKNOWLEDGEMENTS

The support of General Electric, Co., and the guidance of Mr. Al Storace are gratefully acknowledged

REFERENCES

Barrett, L.E., E.J. Gunter, and P.E. Allaire, 1978, "Optimum Bearing and Support Damping for Unbalance Response and Stability of Turbomachinery", ASME *Journal of Engineering for Power*, January 1978, pp.89-94.

Ek, M.C., 1981, "Dynamics Problems in High Performance Rocket Engine Turbomachinery", NASA-Lewis Workshop, February 23, 1981.

Nikolajsen, J.L., and M.S. Hoque, 1990, "An Electroviscous Damper for Rotor Applications", ASME *Journal of Vibrations and Acoustics*, Vol. 112, pp. 440-443.

Den Hartog, J. P., 1930, "Forced Vibrations with Combined Coulomb and Viscous Damping," *ASME Transactions*, 53, APM 107-115.

Den Hartog, J.P., 1956, *Mechanical Vibrations*, 4th Edition, McGraw-Hill, PP.373-377.

Jacobsen, L.S., 1930, "Steady Forced Vibrations as Influenced by Damping," *ASME Transactions*, 52, APM, pp. 169-180.

Kirk, R. G., and E. J. Gunter, 1972, "The Effect of Support Flexibility and Damping on the Synchronous Response of a Single Mass Flexible Rotor," ASME *Journal of Engineering for Industry*, pp. 221-232.

Kollias, A., and A. D. Dimaragonas, 1992, "Damping of Rotor Vibrations Using Electrorheological Fluids in Disc Type Devices", Proceedings of the 3rd International Congress on Adaptive Structures, November 9-11, San Diego, CA, pp. 176-193.

Steidel, R.F., Jr., 1989, *An Introduction to Mechanical Vibrations*, Third Edition, John Wiley & Sons Pubs., pp. 217 – 220.

Timoshenko, S, 1974, *Vibration Problems in Engineering*, McGraw Hill Pubs.

Vance, J.M., 1988, *Rotordynamics of Turbomachinery*, John Wiley & Sons Pubs., pp. 12-17.

Vance, J.M. and D., Ying, 1999, "Experimental Measurements of Actively Controlled Bearing Damping With An Electrorheological Fluid ", presented at the *ASME Turbo-Expo'99 Conference*, Indianapolis, IN, June.

Vance, J.M., D. Z. Ying, D.Z., and J.N. Nikolajsen, 1999, "Actively Controlled Bearing Dampers for Aircraft Engine Applications", presented at the *ASME Turbo-Expo'99 Conference*, Indianapolis, IN, June.

Table 1: Rotor and coulomb damper parameter used for rotor model 1.

Source: test rotor (Vance, Ying and Nicolajsen, 1999)

½ Rigid rotor mass	M_1	17 lb	7.71 kg	Unlocked
½ Flex. rotor mass	M_2	4 lb	1.81 kg	Locked
Support Stiffness	K_1	15000 lb/in	2.62 MN/m	Squirrel cage
Shaft stiffness	K_2	8000 lb/in	1.40 MN/m	Locked support
Viscous damping ratios				
at supports	ζ_1	0.05, 0.25		At zero voltage
at rotor midspan	ζ_2	0.015		Locked support
Unbalance	u	0.0015 in	0.038 mm	Static
Coulomb force	F_C	40 lb	178 N	10 rpm for voltage on
Frequency range		0-10000 rpm	0-1048 rad/sec	7100 rpm for voltage off
Natural frequency	ω_n	5576 rpm	583.9 rad/s	Unlocked support
	ω_s	8395 rpm	879.0 rad/s	Locked support
Break-loose freq.	ω_b	7435 rpm	778.5 rad/s	
Coulomb parameter	$d_C = F_C/ku$	1.78		

Table 2: Flexible rotor-support response (model 2) at critical speeds

$\alpha = 0.25,\ \beta = 0.5,\ \zeta_1 = 0.01,\ \zeta_2 = 0.075$

		r_1			r_2		
d_C	$\overline{\omega}_b$	ω_1	ω_s	ω_2	ω_1	ω_s	ω_2
0.00	0.000	5.054	0.999	3.025	7.216	1.258	1.289
0.25	0.447	2.083	0.999	2.382	3.000	1.311	1.247
0.50	0.577	0.000	0.998	1.738	0.425	1.407	1.214

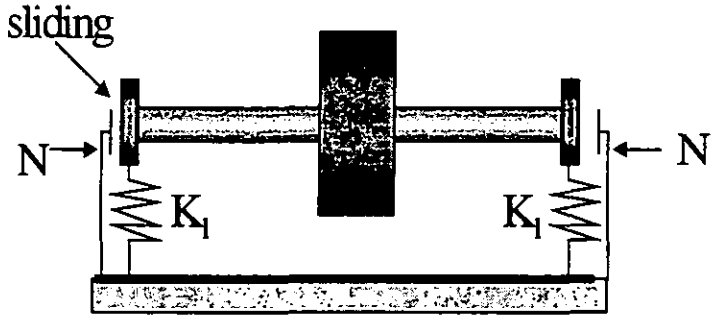

Figure 1. Rigid (Jeffcott) rotor model 1 with Coulomb damping.

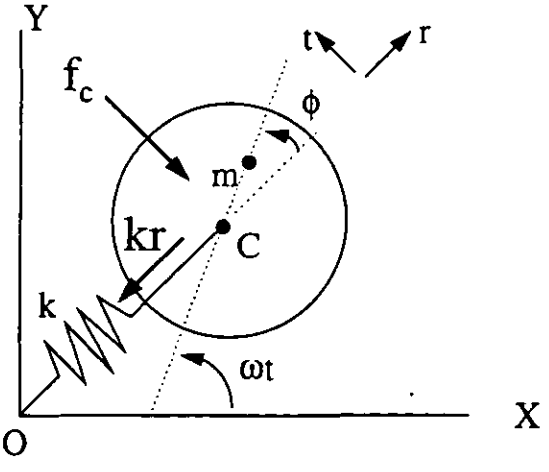

Figure 2: Dynamic force vectors for circular orbits

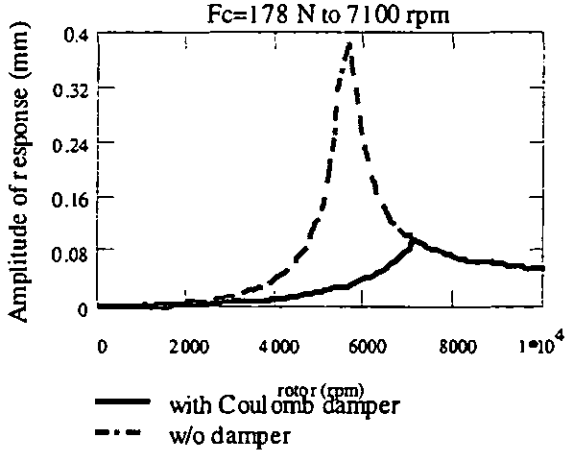

Figure 3. Amplitude of rotor response with Coulomb damper active and without damper (ζ_1=0.05).

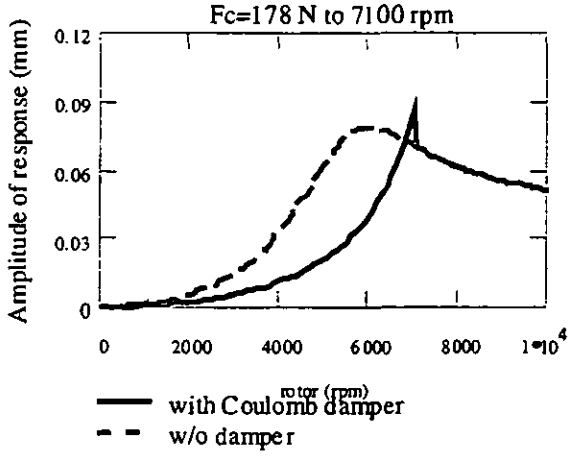

Figure 4. Amplitude of rotor response with Coulomb damper active and without damper (ζ_1=0.25).

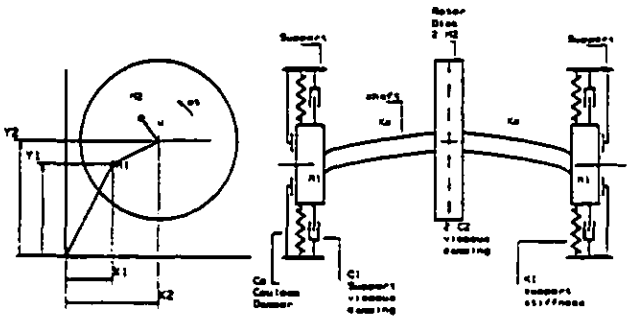

Fig. 5 The rotordynamic model 2 with combined damping.

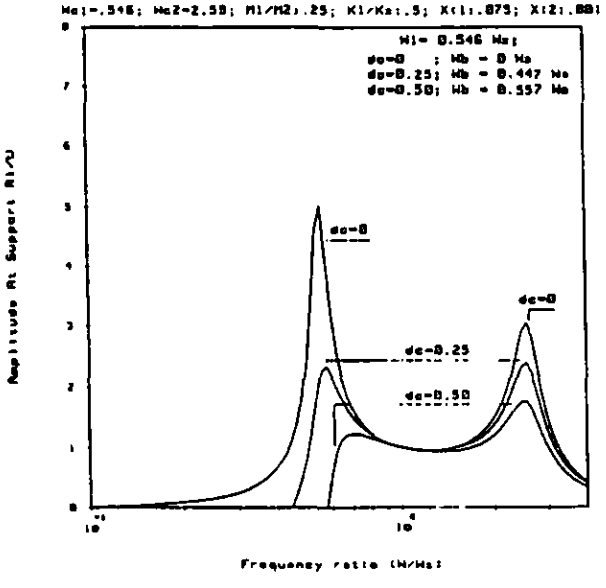

Fig. 6 Unbalance amplitude response at flexible damped supports versus frequency for Coulomb damping parameters d_c = 0.00, 0.25 and 0.50.

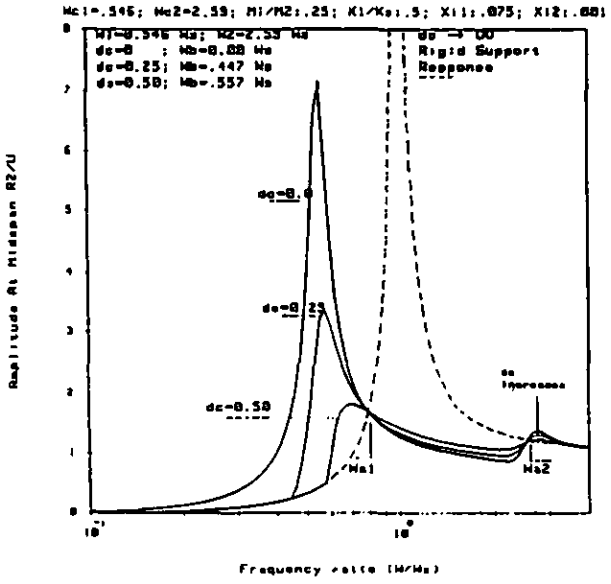

Fig. 7 Unbalance amplitude of midspan versus frequency for Coulomb damping parameters d_c = 0.00, 0.25 and 0.50.

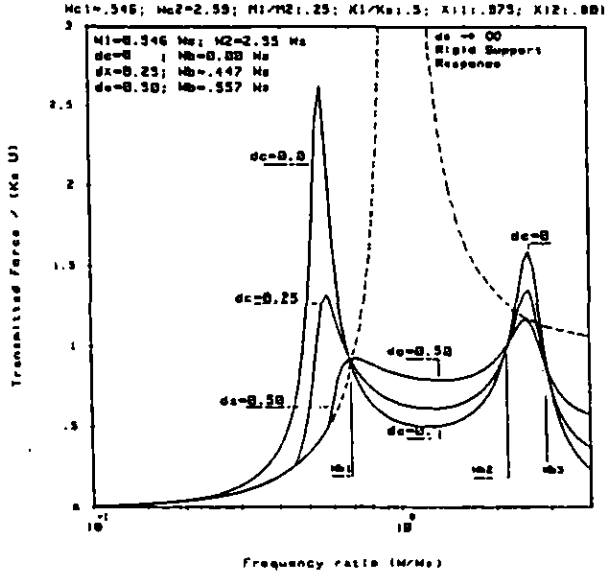

Fig. 8 Amplitude of transmitted force to structure of flexible rotor on damped elastic supports versus frequency for Coulomb damping parameters d_c = 0.00, 0.25 and 0.50.

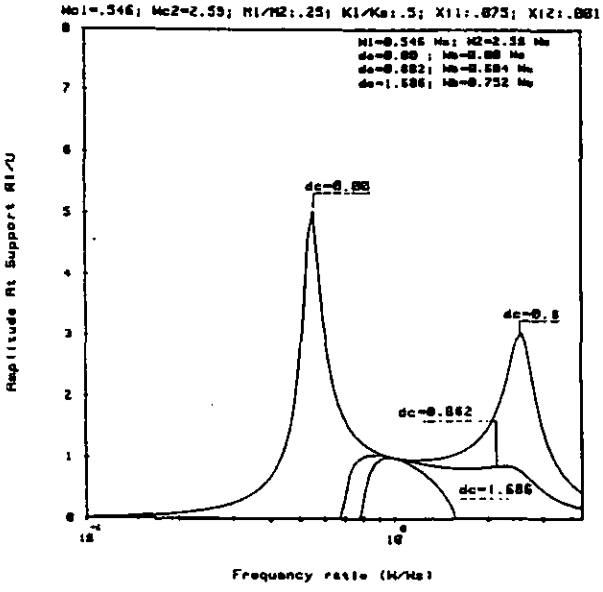

Fig. 9 Unbalance amplitude response at supports versus frequency for optimum values of Coulomb damping parameter d_c = 0.882 and d_c = 1.686.

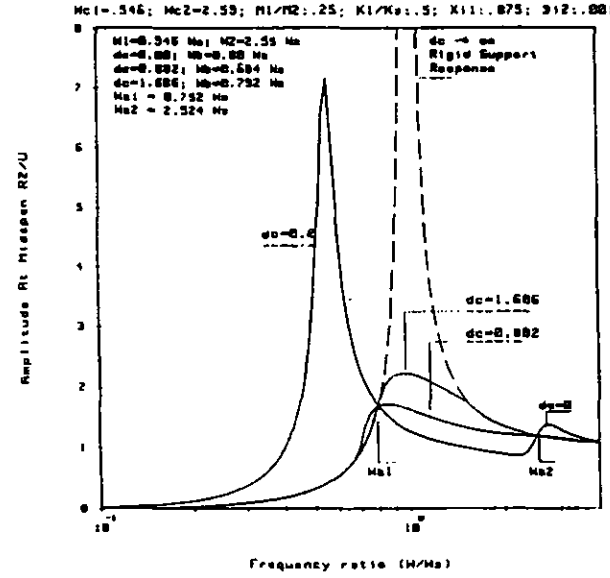

Fig. 10 Unbalance amplitude response at midspan of flexible rotor versus frequency for optimum values of Coulomb damping parameters, d_c = 0.882 for minimum transmitted forces, and d_c = 1.686 for minimum amplitude at midspan.

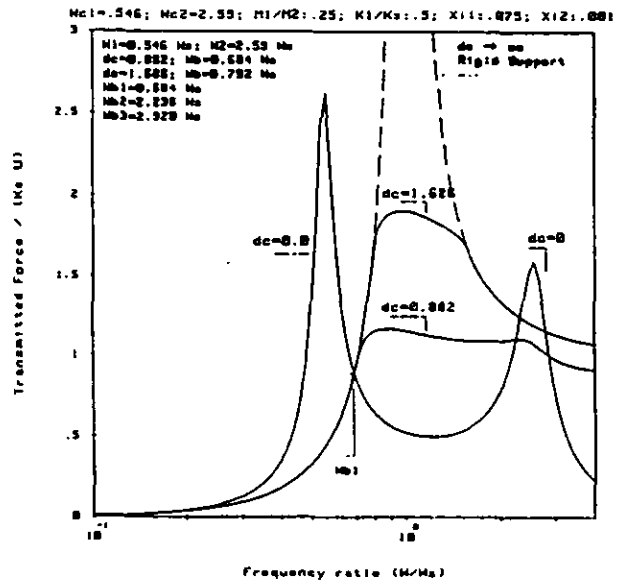

Fig. 11. Amplitude of transmitted force to structure of flexible rotor on damped elastic supports versus frequency. Optimum Coulomb damping parameters d_c = 0.882 and d_c = 1.686.